



AMS
American Meteorological Society

Supplemental Material

[© Copyright 2019 American Meteorological Society](#)

Permission to use figures, tables, and brief excerpts from this work in scientific and educational works is hereby granted provided that the source is acknowledged. Any use of material in this work that is determined to be “fair use” under Section 107 of the U.S. Copyright Act or that satisfies the conditions specified in Section 108 of the U.S. Copyright Act (17 USC §108) does not require the AMS’s permission. Republication, systematic reproduction, posting in electronic form, such as on a website or in a searchable database, or other uses of this material, except as exempted by the above statement, requires written permission or a license from the AMS. All AMS journals and monograph publications are registered with the Copyright Clearance Center (<http://www.copyright.com>). Questions about permission to use materials for which AMS holds the copyright can also be directed to permissions@ametsoc.org. Additional details are provided in the AMS Copyright Policy statement, available on the AMS website (<http://www.ametsoc.org/CopyrightInformation>).

1 **Supporting Information for “Recent warming has resulted in smaller**
2 **gains in net carbon uptake in northern high latitudes”**

3

4 Peng Zhu¹, Qianlai Zhuang^{1,2}, Lisa Welp¹, Philippe Ciais³, Martin Heimann⁴, Bin
5 Peng^{5,6}, Wenyu Li⁷, Carl Bernacchi^{8,9}, Christian Roedenbeck⁴, Trevor F. Keenan¹⁰

6 1. Department of Earth, Atmospheric, and Planetary Sciences, Purdue University,
7 West Lafayette, Indiana 47907 USA

8 2. Department of Agronomy, Purdue University, West Lafayette, Indiana 47907
9 USA

10 3. Laboratoire des Sciences du Climat et de l’Environnement (LSCE), CEA CNRS
11 UVSQ, 91191 Gif-sur-Yvette, France

12 4. Max Planck Institute for Biogeochemistry, 07701 Jena, Germany

13 5. National Center for Supercomputing Applications, University of Illinois at
14 Urbana-Champaign, Urbana, IL 61801, USA

15 6. Department of Natural Resources and Environmental Sciences, University of
16 Illinois at Urbana-Champaign, Urbana, IL 61801, USA

17 7. Ministry of Education Key Laboratory for Earth System Modeling, Tsinghua
18 University, Beijing, China

19 8. Department of Plant Biology, University of Illinois at Urbana-Champaign, Urbana,
20 IL 61801, USA

21 9. Global Change and Photosynthesis Research Unit, USDA-ARS, Urbana, IL 61801,
22 USA

23 10. Earth Sciences Division, Lawrence Berkeley National Lab, Berkeley, California
24 94709, USA

25 Correspondence to: qzhuang@purdue.edu

26

27

28

29

30 **Contents of this file**

31 Tables S1 to S2

32 Figures S1 to S12

33

34 **Prediction of temperature sensitivity of net ecosystem production (NEP) based**
 35 **on conceptual model:**

36 GPP=NEP+ER, where NEP is net ecosystem production and ER is ecosystem
 37 respiration. The temperature sensitivity of each component can be written as:

$$38 \frac{dGPP}{dTsa} = \frac{dNEP}{dTsa} + \frac{dER}{dTsa} \quad (1)$$

39 Here we define NEP/GPP as the ecosystem carbon use efficiency (CUE), then
 40 equation (1) can be written as:

$$41 \frac{dGPP}{GPP \cdot dTsa} = CUE \frac{dNEP}{NEP \cdot dTsa} + (1 - CUE) \frac{dER}{ER \cdot dTsa} \quad (2)$$

42 The standardized temperature sensitivity of GPP ($\sigma_{GPP/Tsa}$), NEP ($\sigma_{NEP/Tsa}$) and ER

43 ($\sigma_{ER/Tsa}$) therefore can be related in equation (2). We used the TP model proposed by

44 Raich et al. to model ER: $ER = ER_{ref} \times f(T) \times f(P)$, where ER_{ref} is the respiration
 45 rate at the reference temperature (T_{ref}), $f(T)$ and $f(P)$ is used to represent of
 46 temperature and precipitation influence. Here we used Arrhenius type equation to

47 model $f(T)$: $f(t) = e^{E_0(\frac{1}{T_{ref}-T_0} - \frac{1}{T-T_0})}$. E_0 is the activation energy parameter and

48 represents the ecosystem respiration sensitivity to temperature. Here we used the
 49 previous study calibrated value (125 K) for evergreen needleleaf forest (Migliavacca
 50 et al., 2011). T_{ref} is fixed at 288.15 K and T_0 is fixed at 227.13 K. Based on this

51 equation, the following equation is obtained: $\sigma_{ER/Tsa} = E_0 / (T - 227.13)^2$. The long

52 term change of summer temperature over the study period increased about 1K, which

53 has a small impact (less than 0.2%/K) on $\sigma_{ER/Tsa}$. The CUE of boreal ecosystem is

54 around 0.1(Luyssaert et al., 2007). Thus if the temporal evolution of CUE and $\sigma_{ER/Tsa}$

55 is ignored, it means 1% change in $\sigma_{GPP/Tsa}$ will cause 10% change in $\sigma_{NEP/Tsa}$. For

56 summer mean temperature is around 14°C (287K). Evaluating equation (2) with

57 $T=287K$, $CUE=0.1$ and $\sigma_{GPP/Tsa} = 2\%$, we get $\sigma_{NEP/Tsa} = -11\%$, where 2%

58 corresponds to a typical temperature sensitivity of GPP in summer according to our
 59 estimation in Fig. 8d. This conceptual analysis implies $\sigma_{NEP/Tsa}$ is very likely to be
 60 negative in summer based on this conceptual framework analysis.

61

62

63

64 Table S1

65

66 Temperature sensitivity of s81 NCE over NHL in the first 17 years (1981-1997) and
 67 the last 17 years (1998-2014) and the corresponding temperature sensitivity of CDR
 68 in the same moving time windows.

69

	1981-1997	1998-2014
$\sigma_{CDR/Tsa}$ in spring	10.2±12% (p>0.1)	-18.5±23% (p>0.1)
$\sigma_{CDR/Tsa}$ in summer	-7.5±7.8% (p>0.1)	-15.1±14% (p<0.05)
$\sigma_{NCE/Tsa}$ in spring	39.4±8.7% (p<0.01)	17.2±12% (p>0.1)
$\sigma_{NCE/Tsa}$ in summer	-8.9±3% (p<0.05)	-14.6±4% (p<0.01)

70

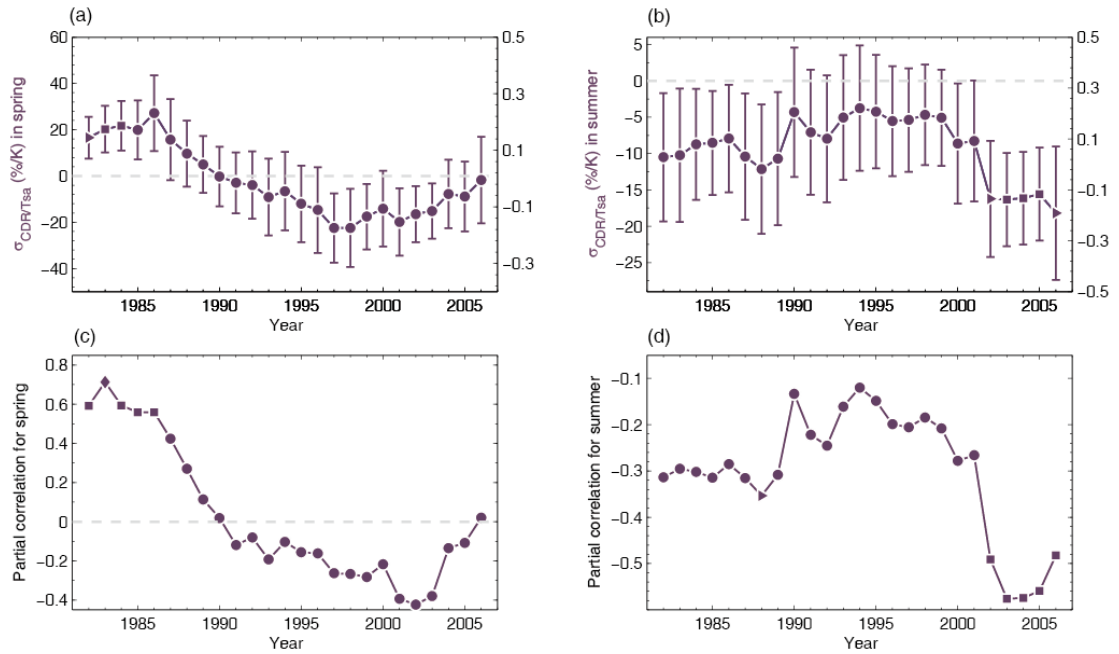
71 Table S2

72 Summary of the nine process-based carbon model in TRENDY project.

Model	Spatial resolution	Vegetation	N-cycle
CLM4CN	1° × 1°	Imposed	Y
LPJ	0.5° × 0.5°	Dynamic	N
LPJGUESS	0.5° × 0.5°	Dynamic	N
OCN	1° × 1°	Imposed	Y
HYLAND	0.5° × 0.5°	Imposed	N
TRIFFD	0.5° × 0.5°	Imposed	N
SDGVM	0.5° × 0.5°	Dynamic	N
VEGAS	0.5° × 0.5°	Dynamic	N
ORCHIDEE	2° × 2°	Imposed	N

73

74



75

76 Figure S1: Temporal evolution of partial correlation between CO₂ drawdown rate and77 Tsa as well as $\sigma_{CDR/Tsa}$ over 17-year moving windows. (a) and (b) shows the78 standardized temperature sensitivity of CDR ($\sigma_{CDR/Tsa}$, %/K). (c) and (d) show the

79 partial correlation between CDR and Tsa in spring and summer when controlling Prec.

80 All of the variables are detrended by its first order difference before doing correlation

81 and regression. Unlike Figure 3, here spring CDR is derived using the end of June as

82 the end of spring and summer CDR is derived using the first day of July as the start of

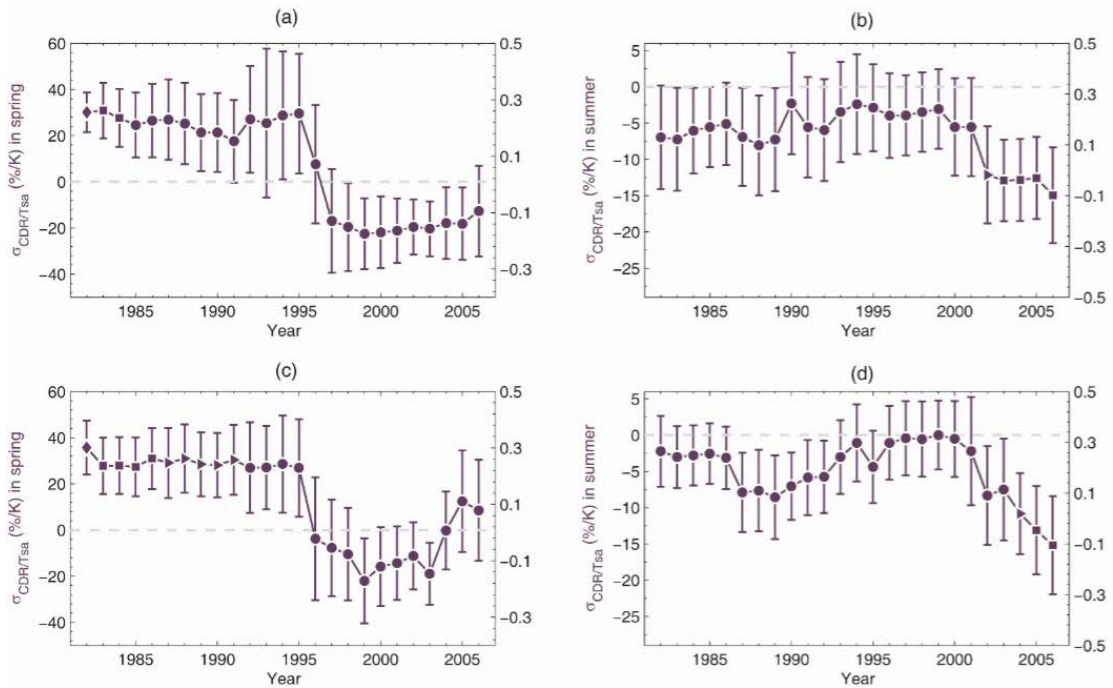
83 summer. The symbols in the line mean the same as the symbols in Figure 3. The error

84 bars indicate the standard errors derived from 17-yr moving windows with bootstrap

85 estimates.

86

87



88

89 Figure S2: Temporal evolution of $\sigma_{CDR/Tsa}$ over 17-year moving windows. (a) and (b)90 shows the standardized temperature sensitivity of CDR ($\sigma_{CDR/Tsa}$, %/K) when not

91 accounting for precipitation and just using temperature as the independent variable in

92 the regression. (c) and (d) show $\sigma_{CDR/Tsa}$ when using the original CDR, Tsa and Prec

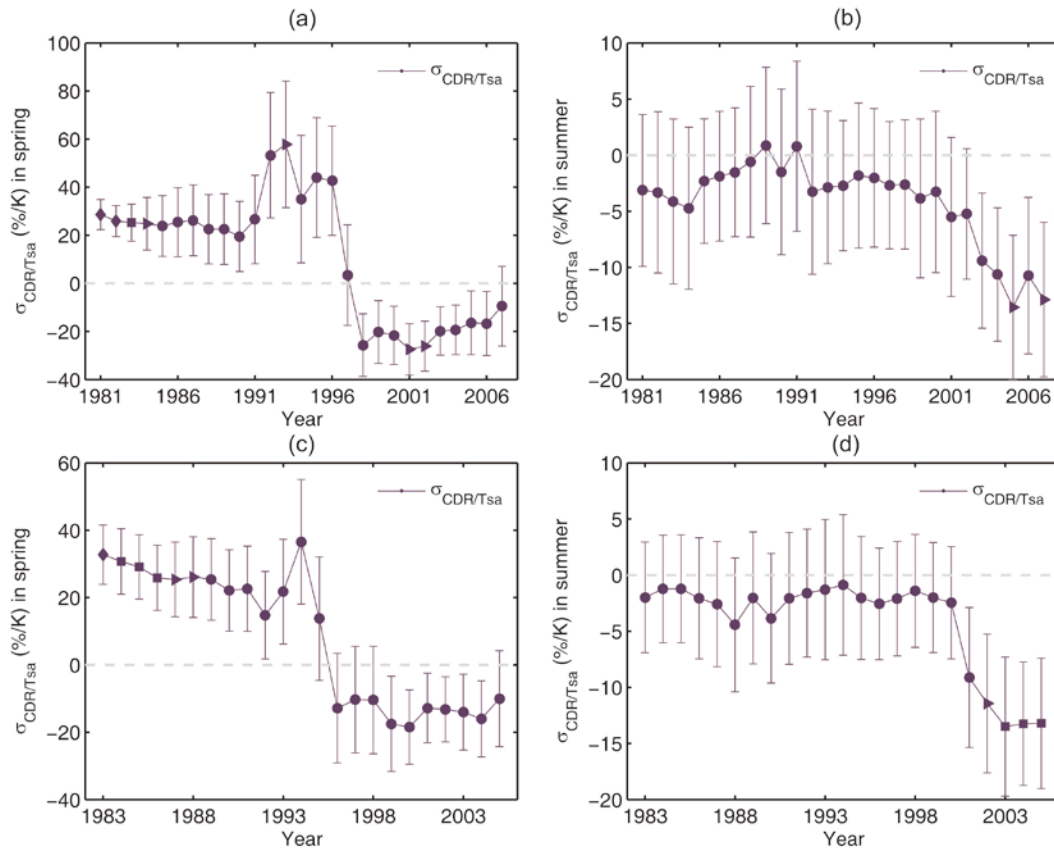
93 without detrending. The symbols in the line mean the same as the symbols in Figure 3.

94 The error bars indicate the standard errors derived from 17-yr moving windows with

95 bootstrap estimates.

96

97



98

99 Figure S3: Temporal evolution of $\sigma_{CDR/Tsa}$ over 15-year moving windows (a,b).100 Temporal evolution of $\sigma_{CDR/Tsa}$ over 19-year moving windows (c,d). The symbols in

101 the line mean the same as the symbols in Figure 3. The error bars indicate the

102 standard errors derived from 17-yr moving windows with bootstrap estimates.

103

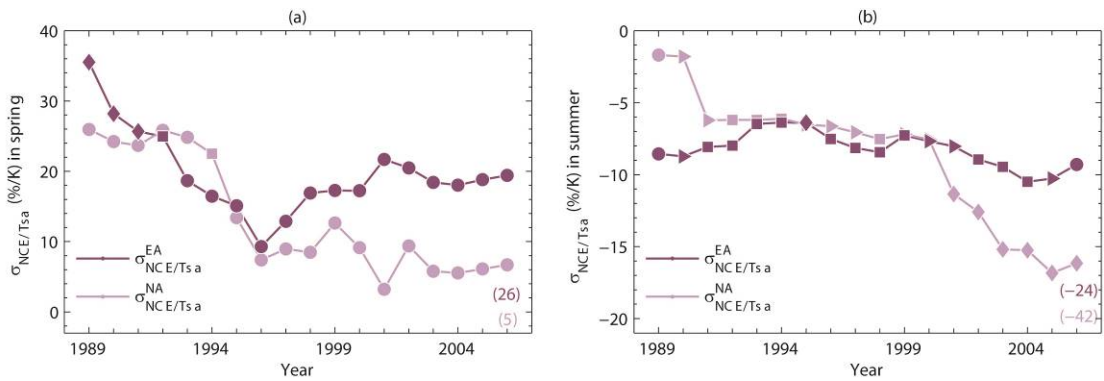
104

105

106

107

108



109

110 Figure S4: Temperature sensitivity of spring (May) and summer $\sigma_{NCE/Tsa}$ (Jul-Aug)

111 using Jena inversion 8.1 carbon exchange in the 17 year windows during

112 1981-2014. When $\sigma_{NCE/Tsa}$ is positive, it means warming will stimulate carbon

113 uptake, otherwise, warming causes carbon loss. NCE data is area weighted over

114 EA and NA along with climate variables. $\sigma_{NCE/Tsa}$ is obtained by regressing

115 detrended NCE over detrended Tsa and detrended Prec and then the regression

116 coefficient is standardized by NCE. Another version of Jena inversion (s99) is also

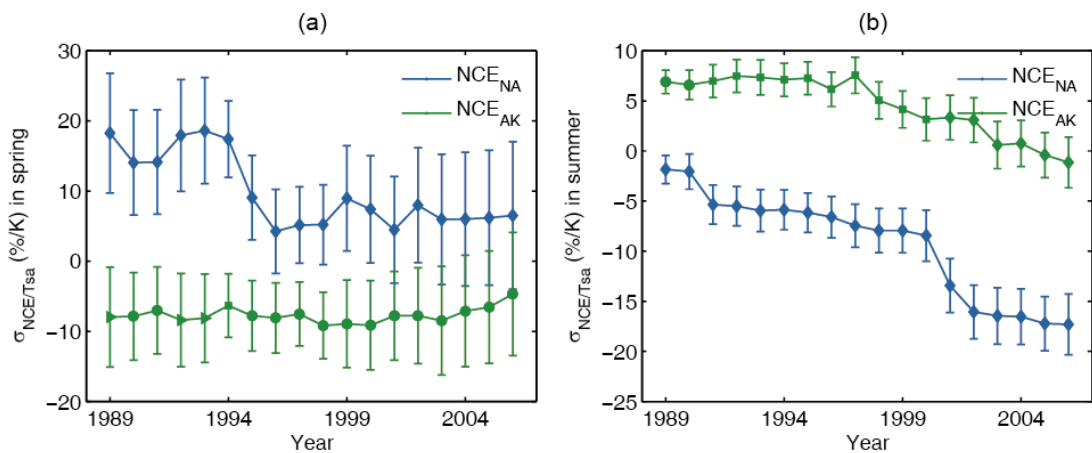
117 employed to show the temperature sensitivity of NCE in the latest 16 years

118 (1999-2014), which is shown as the numbers in parenthesis corresponding to year

119 of 2006.

120

121



122

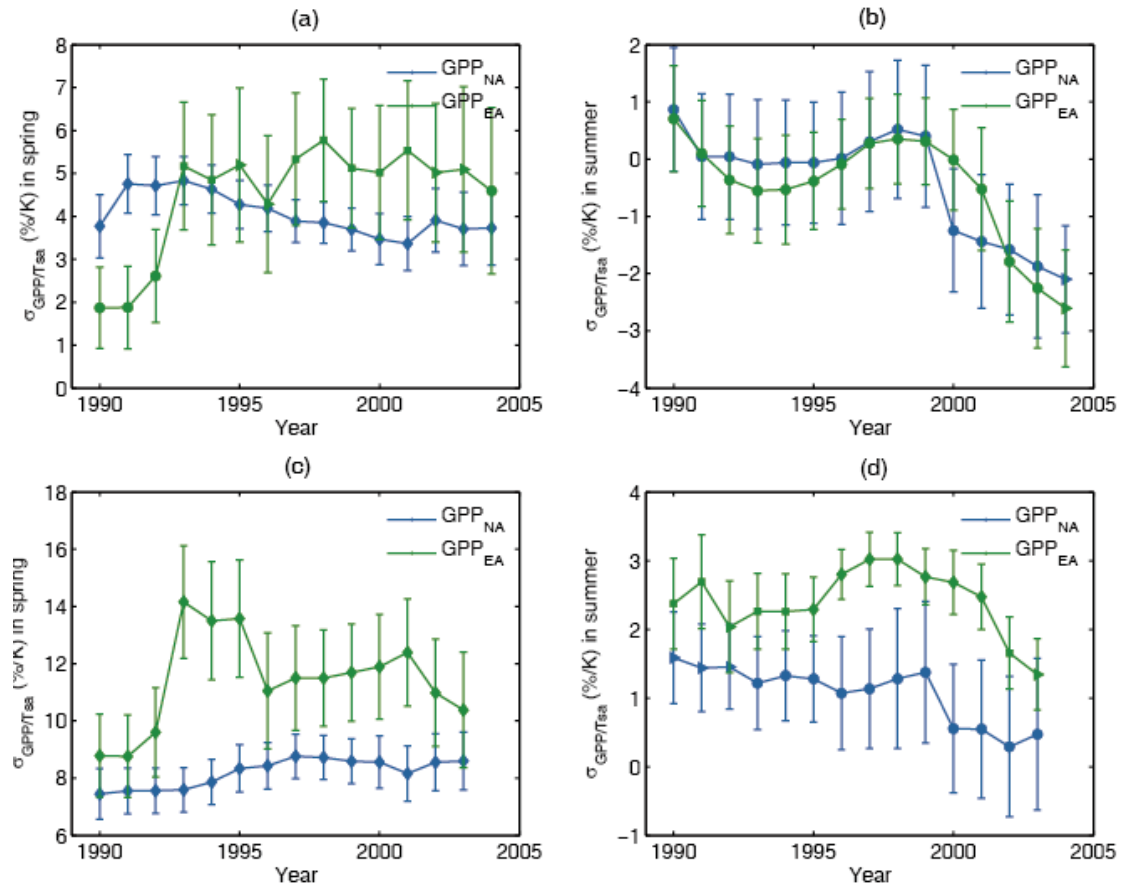
123 Figure S5: When North America continent is further divided into Alaska (AK) and

124 the remaining land (NA) areas, the temperature sensitivity of spring (May) and

125 summer $\sigma_{\text{NCE}/T_{\text{sa}}}$ (Jul-Aug) in the 17 year windows during 1981-2014. NCE data
 126 is area weighted over NA and AK along with climate variables.

127

128



129

130 Figure S6: The temperature sensitivity of spring (May) and summer (Jul-Aug)

131 $\sigma_{\text{GPP}/T_{\text{sa}}}$ from GPP_{LUE} (a,b) and GPP_{MTE} (c,d) in the 17-year windows during

132 1982-2012 over Northern Eurasia and North America. Both GPP_{LUE} GPP_{MTE} and
 133 climate variables are area weighted over vegetated area of Eurasia and North America.

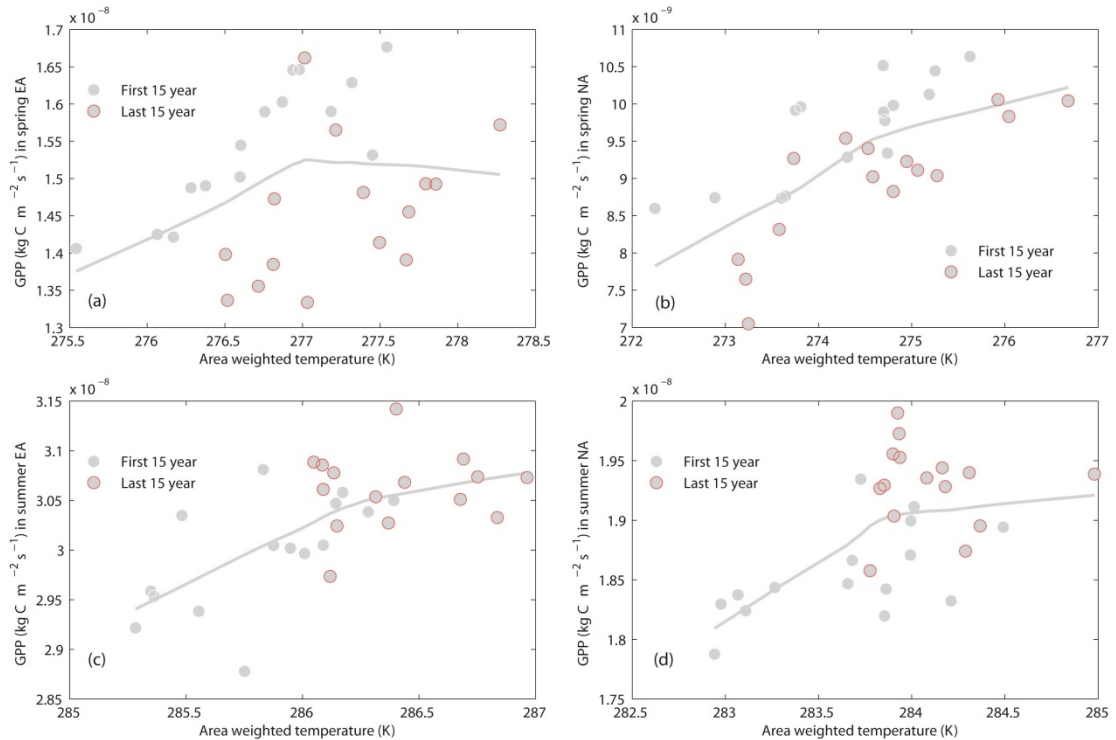
134 The symbols in the line mean the same as the symbols in figure 3. The error bars

135 indicate the standard errors derived from 17-yr moving windows with bootstrap

136 estimates.

137

138



139

140 Figure S7: The spatial mean GPP_{MTE} vs. area weighted temperature for the spring

141 EA (a), spring NA (b), summer EA (c) and summer NA (d) during 1982-2011. The

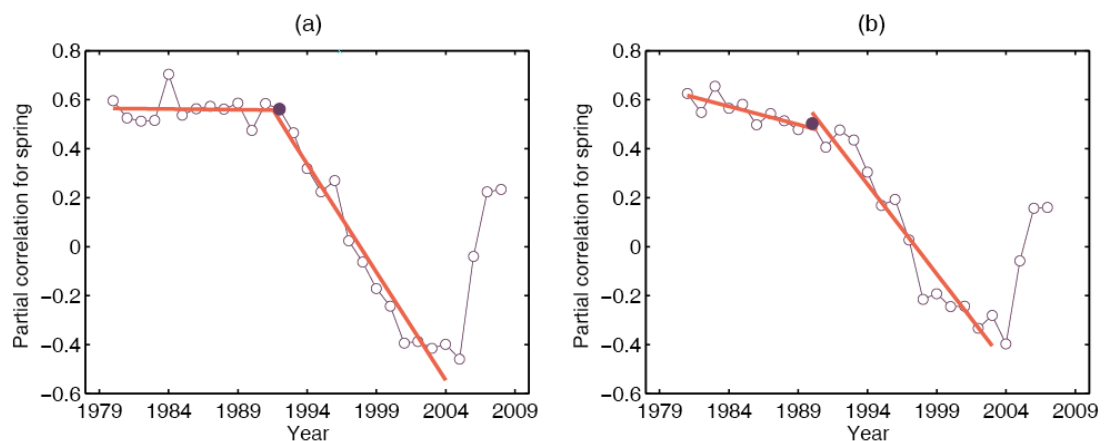
142 first 15 years corresponds to 1982-1996 and last 15 years corresponds to

143 1997-2011. The GPP_{MTE} -temperature response curve is obtained by

144 locally-weighted polynomial regression (LOWESS).

145

146



147

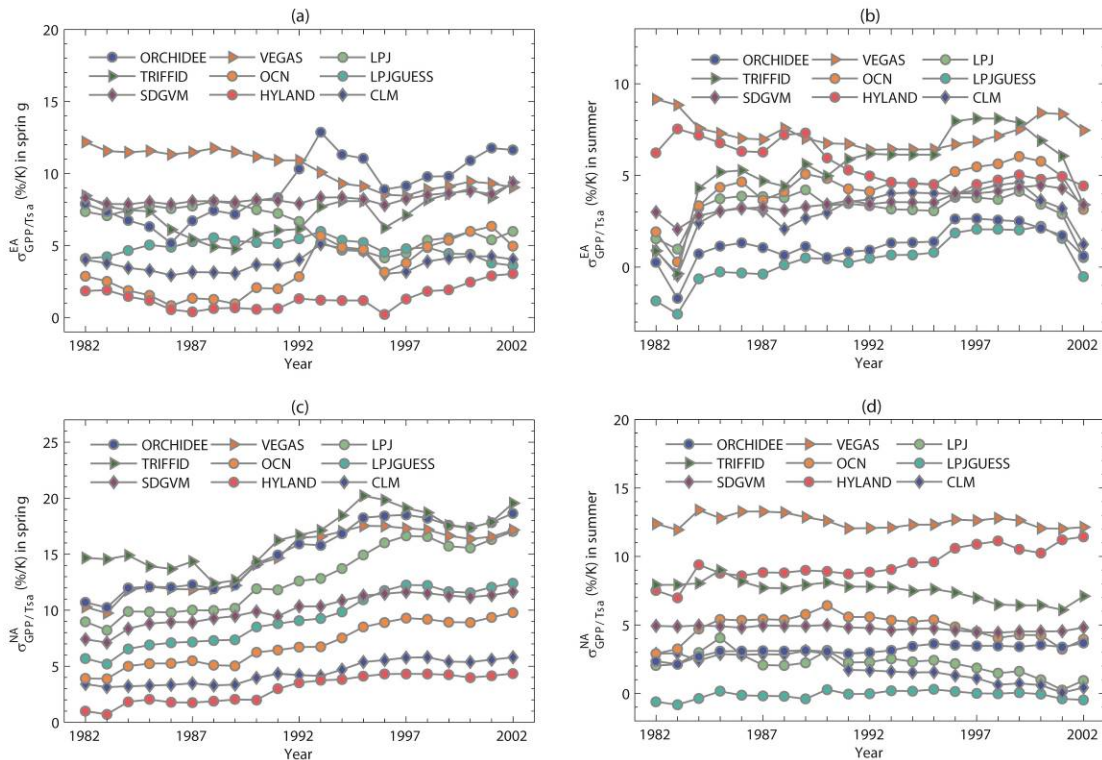
148 Figure S8: Breakpoints in the time series of partial correlation between spring

149 temperature and CDR in 13 years running windows (a) and 15 years running

150 windows (b). The marked point represents the breakpoint. The breakpoint is

151 determined by piece-wise linear model.

152



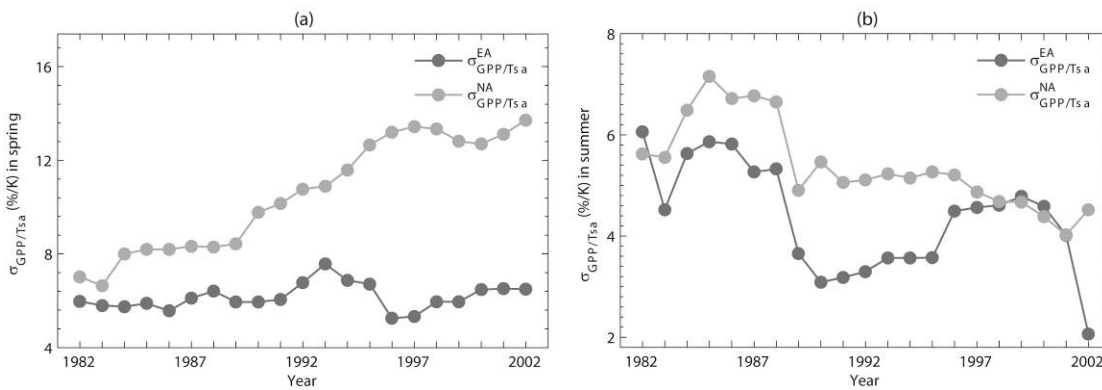
153

154 Figure S9: Temperature sensitivity of spring (a,c) and summer (b,d) GPP $\sigma_{GPP/Tsa}$

155 derived from trendy model results in the 17 year windows during 1974-2010 over the

156 Eurasia (a,b) and North America (c,d).

157



158

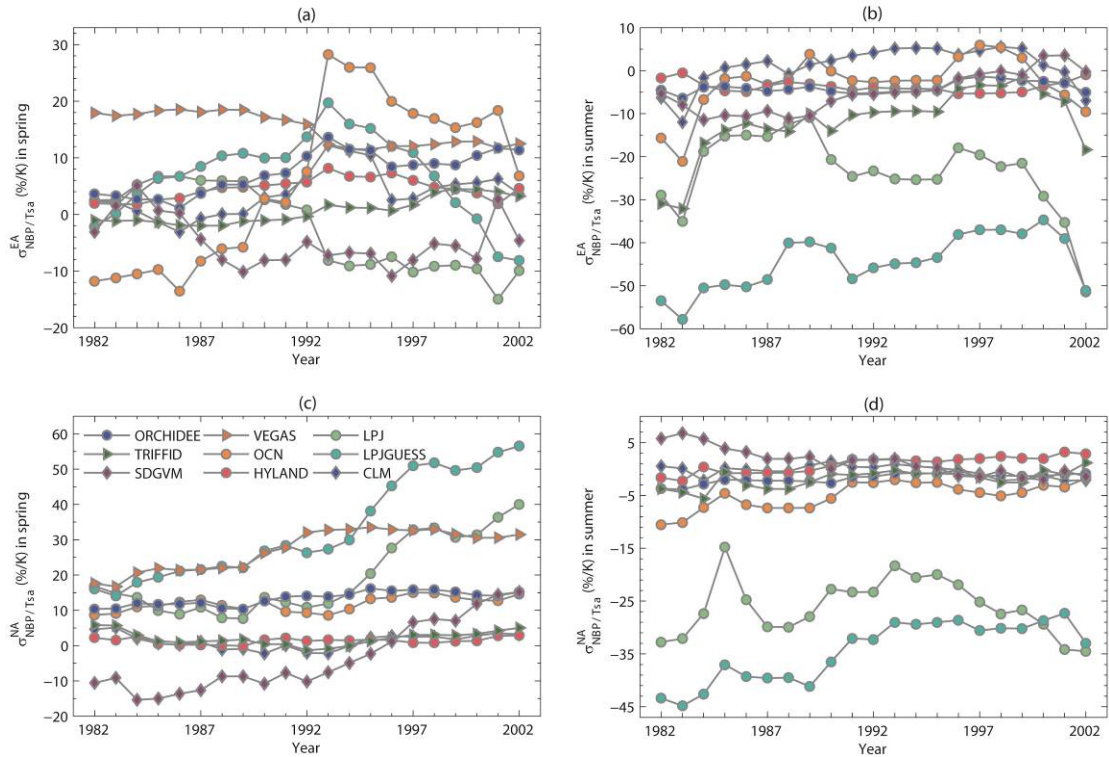
159 Figure S10: Temperature sensitivity of mean spring (a) and summer (b) GPP ($\sigma_{GPP/Tsa}$)

160 by averaging 9 model results from trendy in the 17 year windows during 1974-2010

161 over the Eurasia and North America.

162

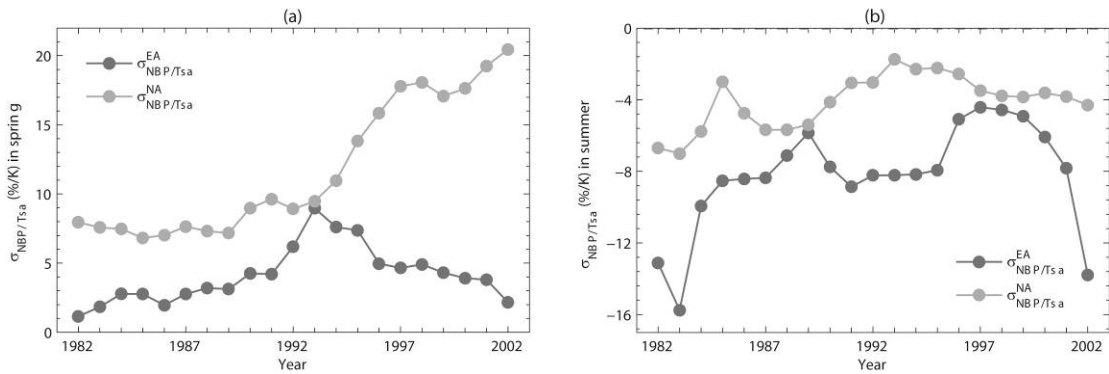
163



164

165 Figure S11: Temperature sensitivity of spring (a,c) and summer (b,d) NBP $\sigma_{NBP/Tsa}$
 166 derived from trendy model results in the 17 year windows during 1974-2010 over the
 167 Eurasia (a,b) and North America (c,d).

168



169

170 Figure S12: Temperature sensitivity of mean spring (a) and summer (b) NBP ($\sigma_{NBP/Tsa}$)
 171 by averaging 9 model results from trendy in the 17 year windows during 1974-2010
 172 over the Eurasia and North America.

173

174

- 175 Migliavacca M, et al. Semiempirical modeling of abiotic and biotic factors controlling
176 ecosystem respiration across eddy covariance sites. *Glob Chang Biol* 17(1):390–409
177 (2011).
- 178 Luysaert, S. et al. Photosynthesis drives anomalies in net carbon-exchange of pine
179 forests at different latitudes. *Global Change Biology* 13, 2110–2127 (2007).
- 180 Raich JW, Potter CS, Bhagawati D. Interannual variability in global soil respiration,
181 1980-94. *Glob Chang Biol* 8(8):800–812 (2002).